PHYSICAL REVIEW B **86**, 195202 (2012)

Evidence of N substitution by Mn in GaN

L. M. C. Pereira,[1,2,3,*] U. Wahl,[2] J. G. Correia,[2] S. Decoster,[1] L. M. Amorim,[1] M. R. da Silva,[4] J. P. Araújo,[3] and A. Vantomme[1]
[1]*Instituut voor Kern-en Stralingsfysica, KU Leuven, 3001 Leuven, Belgium*
[2]*Instituto Tecnológico e Nuclear, Instituto Superior Técnico, Universidade Técnica de Lisboa, 2686-953 Sacavém, Portugal*
[3]*IFIMUP and IN-Institute of Nanoscience and Nanotechnology, Universidade do Porto, 4169-007 Porto, Portugal*
[4]*Centro de Física Nuclear da Universidade de Lisboa, 1649-003 Lisboa, Portugal*

(Received 8 July 2012; revised manuscript received 18 October 2012; published 5 November 2012)

We report on the lattice location of Mn in wurtzite GaN using β^- emission channeling. In addition to the majority substituting for Ga, we locate up to 20% of the Mn atoms in N sites. We propose that the incorporation of Mn in N sites is enabled under sufficiently high concentrations of N vacancies, and stabilized by a highly charged state of the Mn cations. Since N substitution by Mn impurities in wurtzite GaN has never been observed experimentally or even considered theoretically before, it challenges the current paradigm of transition metal incorporation in wide-gap dilute magnetic semiconductors.

DOI: 10.1103/PhysRevB.86.195202 PACS number(s): 75.50.Pp, 61.72.uj, 61.80.Jh, 71.55.Gs

I. INTRODUCTION

Dilute magnetic semiconductors (DMS) continue to challenge our understanding of how transition metal impurities behave in wide-gap nitrides and oxides, both in terms of magnetism and structure.[1] With ferromagnetism being reported well above the ordering temperatures of any other type of dilute magnetic materials, wide-gap DMS still divide the magnetism community between those who report it and those who report its absence (see, e.g., Refs. 1–5 for recent discussions). With respect to structural properties, only in the past few years has a more consistent picture of the structural phase diagram of some wide-gap DMS started to emerge, with phenomena such as spinodal decomposition and other types of chemical and structural phase-segregation being carefully documented (see, e.g., Ref. 1 and references therein). It is, however, at the very basis of the structural and magnetic properties of wide-gap DMS that some of the most puzzling reports can be found: the lattice sites occupied by the transition metal impurities. By determining the impurity electronic structure and the energy barriers that it must overcome in order to diffuse, the impurity lattice site directly controls its magnetism and aggregation behavior. Although it is generally accepted that 3d transition metals such as Mn and Co occupy only cation sites in wide-gap nitrides and oxides (e.g., Ga in GaN and Zn in ZnO), some reports suggest that this is not a general rule (see Ref. 6 for a recent discussion on ZnO).

One of the most well-understood wide-gap DMS, Mn-doped GaN is also one of those that best illustrate the open questions regarding (i) the magnetism, (ii) phase pureness, and (iii) the lattice location of the magnetic impurities. Despite the many reports of ferromagnetism at and above room temperature (i), recent studies on carefully characterized materials found only paramagnetism,[2] antiferromagnetic interactions,[7] or ferromagnetic order with very low Curie temperature ($T_C <$ 10 K).[8] Mn-doped GaN is also an interesting system in which to study "subtle" forms of impurity segregation (ii) using, for example, synchrotron radiation,[9] which can easily pass undetected using more conventional characterization techniques. Regarding the lattice location of the Mn impurities (iii), although the majority of the reports are consistent with cation (Ga) substitution (e.g., based on x-ray absorption fine structure (XAFS),[2,3,10,11] ion channeling,[12,13] and electron channeling[14]), some observations do not completely conform to it. This is particularly the case for zincblende GaN, for which there are strong indications that Mn impurities may occupy non-Ga-substitutional sites. Based on x-ray absorption near edge structure (XANES) measurements, it has been reported that small fractions of the Mn impurities are located on interstitial sites.[15] Based on extended x-ray absorption fine structure (EXAFS) measurements, a remarkably high fraction of 75% of the Mn impurities was found to occupy anion (N) substitutional sites.[16] However, the unambiguous identification of the occupied sites in cases of double occupancy poses a number of challenges to XAFS techniques (EXAFS and XANES). In addition, it is unknown if the non-Ga substitution observed in the zincblende GaN may also occur in wurtzite GaN, which is by far more commonly used in the context of GaN-based applications and DMS.

Here, we report on the lattice location of Mn impurities implanted in epitaxial thin films of wurtzite GaN, using the emission channeling technique. The aim is to determine if and which non-Ga-substitutional sites may be occupied by Mn impurities in the wurtzite lattice, using a technique that has been specifically developed for lattice location of ion implanted impurities in single-crystalline materials. Measurements were carried out in the as-implanted state and after thermal annealing up to 900 °C in order to investigate the thermal stability of the Mn impurities in the respective lattice sites. We focused on the low concentration regime (below 1×10^{19} cm^{-3}, i.e., <0.03%) in order to minimize possible effects of Mn segregation.

II. EXPERIMENT

Emission channeling[17] makes use of the charged particles emitted by a decaying radioactive isotope. The screened Coulomb potential of atomic rows and planes determines the anisotropic scattering of the particles emitted isotropically during decay. Because these channeling and blocking effects strongly depend on the initial position of the emitted particles, they result in angular emission patterns around major crystallographic axes, which are characteristic of the lattice site(s) occupied by the probe atoms. We have previously used the emission channeling technique to determine the lattice location

 ©2012 American Physical Society

of other impurities in GaN (e.g., Fe,[18] As,[19] and several rare earths[20]). The technique is particularly suited in cases where significant fractions of the impurity atoms occupy more than one lattice site. For Mn impurities in particular, this multisite lattice location capability has allowed us to locate a fraction of implanted Mn on the bond-centered (BC) interstitial site in Ge,[21] in anion-substitutional sites (Oxygen sites) in ZnO,[6] as well as to unambiguously identify the interstitial Mn site in GaAs and quantitatively study its thermal stability.[22,23]

Epitaxial thin films of wurtzite [0001] GaN grown on sapphire were implanted at room temperature with a fluence of 2×10^{13} cm^{-2} of radioactive ^{56}Mn ($t_{1/2} = 2.56$ h), at the on-line isotope separator facility ISOLDE at CERN. The implantations were performed under a tilt angle of 17° to minimize ion channeling, using an energy of 50 keV, resulting in a peak concentration of 7×10^{18} cm^{-3} at a projected range of 247 Å with a 114 Å straggling, as estimated using the MARLOWE code.[24] Angular-dependent emission yields of the β^- particles emitted during decay to stable ^{56}Fe were measured at room temperature, along four crystallographic directions, [0001], [$\bar{1}$102], [$\bar{1}$101], and [$\bar{2}$113], in the as-implanted state and after *in situ* capless annealing in vacuum ($<10^{-5}$ mbar) at 300, 600, 700, 800, and 900 °C. The patterns were recorded using a position- and energy-sensitive detection system similar to that described in Ref. 25. Given the short half-life of ^{56}Mn, this system was installed online and upgraded with self-triggering readout chips for the Si pad detectors, enabling measurements during and/or immediately after implantation with count rates of up to several kHz.

III. RESULTS

Quantitative lattice location is provided by fitting the two-dimensional experimental patterns with theoretical ones using the fit procedure outlined in Ref. 26. The theoretical patterns were calculated using the *many-beam* formalism[17] for probes occupying various sites in the wurtzite GaN structure:[27] substitutional Ga (S_{Ga}) and N (S_N) sites with varying root-mean-square displacements, the main interstitial sites, i.e., tetrahedral (T), octahedral (O), hexagonal (H), bond-centered (BC), and antibonding (AB), as well as interstitial sites resulting from displacements along the *c* or the basal directions. For all four measured directions, the calculated S_{Ga} patterns gave by far the best agreement, showing that the majority of the probe atoms occupy S_{Ga} sites, as expected. The fitting routine was then allowed to include, in addition to S_{Ga}, an additional lattice site, for which all simulated sites were considered. Consistently for all measured directions, the $S_{Ga} + S_N$ double occupancy gave the best fit compared to all other combinations and considerably improves the S_{Ga} single-site fit. This is illustrated in Fig. 1(a), which shows the reduced χ^2 of the fit as the non-S_{Ga} site is moved along the *c* axis between two neighboring S_{Ga} sites (the [0001] direction is not included since it does not distinguish sites along the *c* axis[6]). Consistently for all three directions, the best fits are centered at the S_N site. The sensitivity of the fit (in terms of magnitude and "width" of the improvement in χ^2) is correlated with the spatial separation between Ga and N rows along the channeling axis (Fig. 1), being most pronounced for the [$\bar{2}$113] direction. For comparison, Fig. 1(b) shows an equivalent χ^2

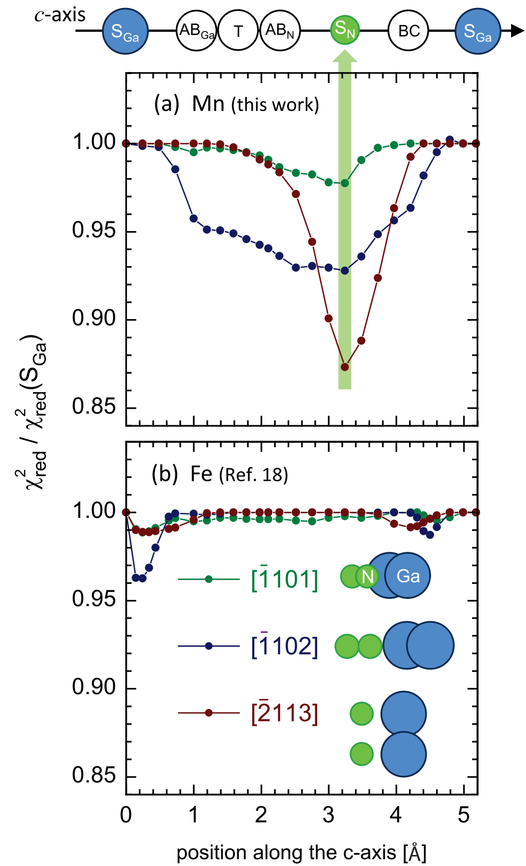

FIG. 1. (Color online) Reduced χ^2 of the fits to the experimental emission yields in the vicinity of the [$\bar{1}$102], [$\bar{1}$101], and [$\bar{2}$113] directions (following 600 °C annealing), for (a) ^{56}Mn (this work) and ^{59}Fe (Ref. 18). Each data point corresponds to the best fit obtained using two given sites, with the corresponding two fractions as free parameters. The site pairs are composed of S_{Ga} plus each of the simulated sites along the *c* axis (depicted above the plot): the S_N and the T sites, the BC and AB sites along the *c* axis, and a number of intermediate positions. The *x* axis corresponds to the position (along the *c* axis) of the non-S_{Ga} site used in each fit. The reduced χ^2 (*y* axis) of these two-site fits are normalized to that of the one-site (S_{Ga}) fit. The nonequivalent rows of Ga and N atoms, projected on the plane perpendicular to each of the axes, are also shown (right). Note that the separation between Ga and N rows is maximized along the [$\bar{2}$113] axis.

plot for ^{59}Fe in GaN, obtained by re-analyzing the data of Ref. 18 using new simulations, which include the same lattice sites as in the case of ^{56}Mn. No discernible decrease in χ^2 is observed around the S_N site. Instead, the data indicates that a fraction of the ^{59}Fe impurities occupy S_{Ga} sites, which are displaced from the the ideal S_{Ga} position by ~0.2 Å (consistent with the analysis in Ref. 18), which indicates the presence of neighboring defects such as N vacancies.

As an example of the good match between experiment and simulated patterns, Fig. 2 compares the normalized experimental β^- emission yields following annealing at 600 °C, along the four measured directions [(a)–(d)] with the best fits of theoretical patterns [(e)–(h)]. The best fit is obtained for 81% of the ^{56}Mn atoms on S_{Ga} (Mn_{Ga}) and 19% on S_N sites (Mn_N). Introducing a third site yields only insignificant fit improvements. Possible fractions in other sites are estimated

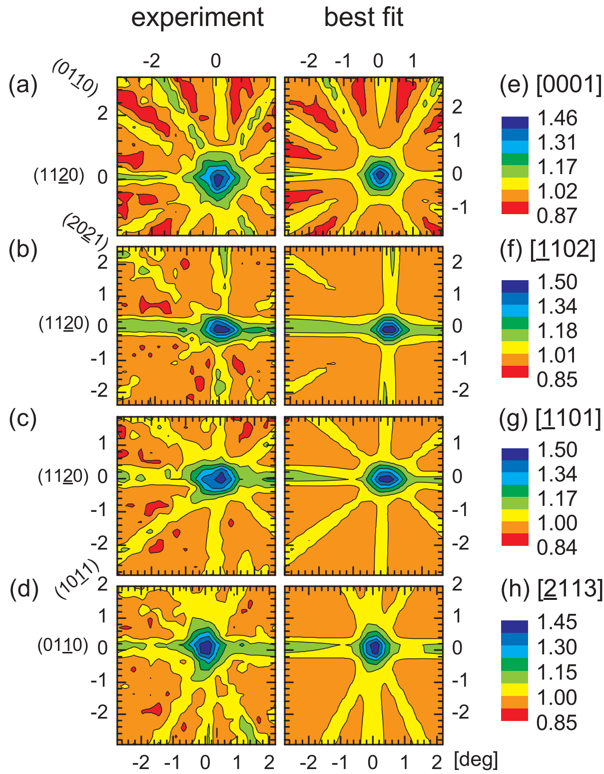

FIG. 2. (Color online) (a)–(d) Normalized experimental ^{56}Mn β^- emission channeling patterns in the vicinity of the [0001], [$\bar{1}$102], [$\bar{1}$101], and [$\bar{2}$113] directions following annealing at 600 °C. (e)–(h) Corresponding best fits with 81 % and 19% of the ^{56}Mn atoms on S_{Ga} and S_N sites, respectively.

to be below 5%. Figure 3 shows the fractions of ^{56}Mn probes in S_{Ga} and S_N sites as a function of annealing temperature. Within the experimental error, the Mn_N fraction remains constant around 20%, up to highest annealing temperature of 900 °C.

IV. DISCUSSION

Chemically, 3d transition metals such as Mn are much more similar to Ga (a post-transition metal) than they are to N (a nonmetal). In particular, the electronegativity and ionic radii of Mn are much closer to those of Ga than N, which in principle makes it energetically unfavorable for Mn impurities to be incorporated in N sites. Because anion substitution by 3d transition metals in GaN is so unexpected, theoretical considerations of the phenomena are very scarce, especially for wurtzite

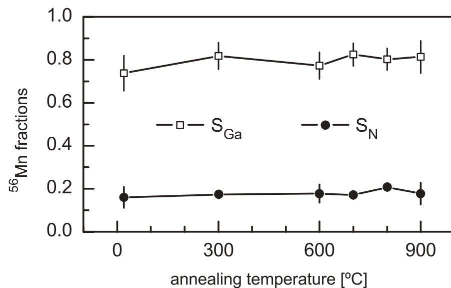

FIG. 3. Fractions of ^{56}Mn impurities on S_{Ga} and S_N sites following each annealing step.

GaN. For zincblende GaN, the calculated total energies for Mn in Ga and N sites indicate, as expected, that Ga substitution is more favorable.[28] However, the calculations in Ref. 28 do not consider charged Mn_N defects. The defect that most resembles Mn_N, for which different charge states have been considered, is the Ga antisite (Ga_N). It has been shown that varying the charge state from neutral to 4+ considerably decreases the formation energy of Ga_N in wurtzite GaN (from ∼8 to ∼1 eV, under Ga-rich/N-poor conditions).[29] Such highly charged states are only stable for a Fermi level sufficiently close to the valence band, i.e., in the presence of acceptor states to which the Ga_N electrons can be transferred. In Mn-doped GaN, that role can be played by the deep acceptor levels of Mn_{Ga} defects (the Ga-substitutional fraction). On the other hand, the requirement of N-poor growth is in agreement with Ref. 16. There, N substitution by Mn (in zincblende GaN) was only observed in thin films grown under N-poor conditions. In other words, increasing the concentration of N vacancies (which can be "filled" by Mn impurities), decreases the formation energy of Mn_N defects. In the present study, the required N vacancies were in principle created upon $^{56}Mn^+$ ion bombardment. Note, nonetheless, that the incorporation of Mn impurities in N sites cannot be considered a direct effect of ion implantation, since it was not observed for Fe under very similar experimental conditions.[18] Fe is a 3d transition metal as well, with an atomic mass that is similar to that of Mn and, therefore, has similar incorporation kinetics. A more detailed description of the conditions under which N substitution by Mn impurities occurs in wurtzite GaN will require the assessment of the formation energies of such defects, as well as an experimental reassessment of the lattice location of Mn in GaN for different preparation methods and growth conditions, carefully taking into consideration the possibility of anion substitution.

Together with our recent report on O-substitutional Mn and Co in ZnO,[6] these results suggest that anion substitution by 3d transition metals may be a general phenomenon in wide-gap nitrides and oxides. However, because it is both highly unexpected and difficult to detect with conventional techniques, anion substitution by transition metals may have so far passed undetected. Although there is no obvious reason to consider anion substitution as a potential route toward room temperature ferromagnetism, a comprehensive description of the phenomenon is fundamental for the understanding of wide-gap DMS. For example, it has been predicted that electron delocalization increases the range of the magnetic interactions between anion-substitutional compared to cation-substitutional Mn impurities in zincblende GaN, potentially leading to spin-glass behavior in anion-substituted Ga(Mn,N).[28] Indeed, magnetometry measurements indicate that while cation-substituted (Ga,Mn)N is not ferromagnetic down to 5 K, anion-substituted Ga(Mn,N) displays some degree of magnetic irreversibility at low temperatures.[16]

In a slightly different context, because anion-substitutional transition metals are likely to behave as donors (as discussed above), they may also play an important role in terms of electrical (self-)compensation. Particularly in Mn-doped GaN, it is relatively well established that the type of magnetic interactions between Ga-substitutional Mn moments is determined by the Mn charge state, which in turn depends

on the concentration of compensating donor defects.[3] Under stringent growth conditions that minimize the concentration of compensating donors such as N vacancies and H impurities, Mn impurities are incorporated as Mn^{3+}. In such cases, ferromagnetic interactions[3] and low temperature order ($T_C <$ 10 K)[8] can be observed. More commonly, such stringent growth conditions are not satisfied and Mn impurities are incorporated as compensated Mn^{2+}, for which only nearest-cation-neighbor antiferromagnetic interactions are observed.[3,7] Being a potential donor defect, Mn_N may also compensate Mn^{3+}_{Ga} impurities, i.e., turning ferromagnetically interacting Mn^{3+}_{Ga} into antiferromagnetically interacting Mn^{2+}_{Ga}. Such electric and magnetic self-compensation by N-substitutional Mn in GaN is very similar to that of interstitial Mn in GaAs, also a donor that compensates acceptor and ferromagnetically interacting Ga-substitutional Mn.[30]

V. CONCLUSION

We have experimentally demonstrated that, in addition to the majority substituting for the cation (Ga), minority fractions (up to 20%) of ion-implanted Mn impurities occupy anion (N) sites in wurtzite GaN. Both Ga- and N-substitutional fractions are virtually unaffected by thermal annealing up to 900 °C. Together with recent reports on anion substitution by Mn and Co in ZnO, these results challenge the current paradigm of transition metal incorporation in wide-gap nitrides and oxides, with profound implications on our understanding of magnetic interactions and self-compensation effects in wide-gap DMS.

ACKNOWLEDGMENTS

This work was supported by the Portuguese Foundation for Science and Technology (CERN/FP/116320/2010, CERN/FP/123585/2011, SFRH/BD/35761/2007), the European Union Seventh Framework through ENSAR (European Nuclear Science and Applications Research, Contract No. 262010), and SPIRIT (Support of Public and Industrial Research Using Ion Beam Technology, Contract No. 227012), the Fund for Scientific Research Flanders, KU Leuven Project No. GOA/2009/006, and the IUAP (Interuniversity Attraction Poles) P6/42 program.

*lino.pereira@fys.kuleuven.be

[1] T. Dietl, Nat. Mater. **9**, 965 (2010).
[2] W. Stefanowicz *et al.*, Phys. Rev. B **81**, 235210 (2010).
[3] A. Bonanni *et al.*, Phys. Rev. B **84**, 035206 (2011).
[4] L. M. C. Pereira, T. Som, J. Demeulemeester, M. J. Van Bael, K. Temst, and A. Vantomme, J. Phys.: Condens. Matter **23**, 346004 (2011).
[5] L. M. C. Pereira, J. P. Araujo, M. J. Van Bael, K. Temst, and A. Vantomme, J. Phys. D **44**, 215001 (2011).
[6] L. M. C. Pereira, U. Wahl, S. Decoster, J. G. Correia, L. M. Amorim, M. R. da Silva, J. P. Araujo, and A. Vantomme, Phys. Rev. B **84**, 125204 (2011).
[7] S. Granville, B. J. Ruck, F. Budde, H. J. Trodahl, and G. V. M. Williams, Phys. Rev. B **81**, 184425 (2010).
[8] E. Sarigiannidou, F. Wilhelm, E. Monroy, R. M. Galera, E. Bellet-Amalric, A. Rogalev, J. Goulon, J. Cibert, and H. Mariette, Phys. Rev. B **74**, 041306 (2006).
[9] G. Martinez-Criado, A. Somogyi, S. Ramos, J. Campo, R. Tucoulou, M. Salome, J. Susini, M. Hermann, M. Eickhoff, and M. Stutzmann, Appl. Phys. Lett. **86**, 131927 (2005).
[10] O. Sancho-Juan, G. Martinez-Criado, A. Cantarero, N. Garro, M. Salome, J. Susini, D. Olguin, S. Dhar, and K. Ploog, Phys. Rev. B **83**, 172103 (2011).
[11] N. Smolentsev, G. Smolentsev, S. Wei, and A. V. Soldatov, Physica B **406**, 2843 (2011).
[12] C. Liu, E. Alves, A. Ramos, M. da Silva, J. Soares, T. Matsutani, and M. Kiuchi, Nucl. Instrum. Methods Phys. Res., Sect. B **191**, 544 (2002).
[13] S. Kuroda, S. Marcet, E. Bellet-Amalric, J. Cibert, H. Mariette, S. Yamamoto, T. Sakai, T. Ohshima, and H. Itoh, Phys. Status Solidi A **203**, 1724 (2006).
[14] T. Niermann, D. Mai, M. Roever, M. Kocan, J. Zenneck, J. Malindretos, A. Rizzi, and M. Seibt, J. Appl. Phys. **103**, 073520 (2008).
[15] S. Wei, W. Yan, Z. Sun, Q. Liu, W. Zhong, X. Zhang, H. Oyanagi, and Z. Wu, Appl. Phys. Lett. **89**, 121901 (2006).
[16] F. Takano, H. Ofuchi, J. Lee, K. Takita, and H. Akinaga, Physica B **376**, 658 (2006).
[17] H. Hofsäss and G. Lindner, Phys. Rep. **201**, 121 (1991).
[18] U. Wahl, A. Vantomme, G. Langouche, J. G. Correia, and L. Peralta, Appl. Phys. Lett. **78**, 3217 (2001).
[19] U. Wahl, J. G. Correia, J. P. Araujo, E. Rita, J. C. Soares, and ISOLDE Collaboration, Appl. Phys. Lett. **90**, 181934 (2007).
[20] U. Wahl, E. Alves, K. Lorenz, J. G. Correia, T. Monteiro, B. De Vries, A. Vantomme, and R. Vianden, Mater. Sci. Eng. B **105**, 132 (2003).
[21] S. Decoster, S. Cottenier, U. Wahl, J. G. Correia, L. M. C. Pereira, C. Lacasta, M. R. Da Silva, and A. Vantomme, Appl. Phys. Lett. **97**, 151914 (2010).
[22] L. M. C. Pereira, U. Wahl, S. Decoster, J. G. Correia, M. R. da Silva, A. Vantomme, and J. P. Araujo, Appl. Phys. Lett. **98**, 201905 (2011).
[23] L. M. C. Pereira, U. Wahl, S. Decoster, J. G. Correia, L. M. Amorim, M. R. da Silva, J. P. Araujo, and A. Vantomme, Phys. Rev. B **86**, 125206 (2012).
[24] M. T. Robinson, Phys. Rev. B **40**, 10717 (1989).
[25] U. Wahl *et al.*, Nucl. Instrum. Methods Phys. Res., Sect. A **524**, 245 (2004).
[26] U. Wahl, J. G. Correia, S. Cardoso, J. G. Marques, A. Vantomme, G. Langouche, and ISOLDE Collaboration, Nucl. Instrum. Methods Phys. Res., Sect. B **136**, 744 (1998).
[27] U. Wahl, A. Vantomme, G. Langouche, J. P. Araújo, L. Peralta, and J. G. Correia, J. Appl. Phys. **88**, 1319 (2000).
[28] C. Y. Fong, V. A. Gubanov, and C. Boekema, J. Electron. Mater. **29**, 1067 (2000).
[29] S. Limpijumnong and C. G. Van de Walle, Phys. Rev. B **69**, 035207 (2004).
[30] T. Jungwirth *et al.*, Phys. Rev. B **72**, 165204 (2005).